Springer

KSME

Journal of Mechanical Science and Technology 29 (12) (2015) 5127~5132
www.springerlink.com/content/1738-494x(Print)/1976-3824(Online)
DOI 10.1007/s12206-015-1111-0

An investigation into the anti-releasing performance of a serrated bolt †

Jin Hwan Jeong[1], Hyun-Kyu Lee[1], Keun Park[2] and Jong-Bong Kim[3,*]

[1]*Dept. Automotive Engng., Seoul Nat'l. Univ. Sci. Technol., Nowon-gu, Seoul, 139-743, Korea*
[2]*Dept. Mech. System Design Engng., Seoul Nat'l. Univ. Sci. Technol., Nowon-gu, Seoul, 139-743, Korea*
[3]*Dept. Mech. and Automotive Engng., Seoul Nat'l. Univ. Sci. Technol., Nowon-gu, Seoul, 139-743, Korea*

(Manuscript Received June 2, 2015; Revised July 17, 2015; Accepted July 27, 2015)

Abstract

As the sizes of electric products, such as mobile phones and watch phones, decrease, the joining bolt for the electric product should also be miniaturized. However, the miniature-sized bolt has to support sufficient joining torque and joining force. The bolt also has to support sufficient anti-releasing torque to keep the product fastened. We investigated a serrated bolt as a candidate for a miniature-sized fastener to increase the anti-release torque. In the serrated bolt, serration shapes are formed on the bottom surface of a bolt head to create an obstacle to releasing. In this study, finite element analyses were carried out on joining and releasing, and the anti-release torque was predicted. Through the joining and releasing analyses for various values of the elastic modulus and yield strength of the joined part, the effect of the mechanical properties of the joined part on the anti-releasing performance were investigated. The analysis results showed that a high strength insert nut is needed to increase the anti-releasing torque when the yield strength of the joined part is low, such as a plastic board in a mobile phone.

Keywords: Serrated bolt; Anti-release torque; Fastener

1. Introduction

With the request for thinner electric products, such as mobile phones and watch phones, the size of the joining bolt must also be decreased [1]. When decreasing the size of the joining bolt, sufficient fastening torque should be provided. Hong et al. [2] and Guo et al. [3] studied the fastening conditions of bolted structures. Chemical adhesive is sometimes used [4] to maintain anti-releasing torque. However, the chemical adhesive techniques have some difficulties in being applied to a subminiature-sized bolt due to a dimensional inaccuracy. Many studies have been carried out to improve the joining or anti-releasing torque, [5-11]. Min et al. [5] and Lee et al. [6] evaluated the effect of thread angle and bit depth, respectively, on joining performance. Sase et al. [7, 8] measured the anti-loosening performance of screw threads, spring washers, nylon-inserted nuts, double nuts, and eccentric nuts under vibratory conditions. Bhattacharya et al. [9] also tested the anti-loosening characteristics of various types of fasteners under vibratory conditions. They showed the serrated bolt has a good anti-loosening performance together with the chemical lock bolt. Pai and Hess [10] and Izumi et al. [11] used finite element analysis to investigate the loosening failure under dynamic loads.

In this study, a serrated bolt is considered a candidate to generate a sufficient anti-releasing performance. In the serrated bolt, serration shapes are formed on the bottom side of a bolt head to prevent easy release of the bolt. In this study, we numerically investigated the anti-releasing performance of a serration bolt. When the joining target material is soft, the serrated bolt will have a good performance, because the serration shape will penetrate into the target material. When the target material has a hard surface, however, the effect of the serration shape will decrease, because the serration shape cannot penetrate into the target materials. Finite element analyses were carried out for various values of Young's modulus and the yield strength. From the analysis results, the effect of the mechanical parameters on the anti-releasing performance of the serrated bolt was investigated. To compare quantitatively the anti-releasing performance of a serrated bolt, the releasing torque of a flat bolt without serration was calculated. Finally, the conditions under which the serrated bolt is effective were determined.

2. Finite element model

Joining and releasing processes of the serrated bolt are analyzed by a three-dimensional Finite element (FE) method. Fig.

*Corresponding author. Tel.: +82 2 970 6434, Fax.: +82 2 979 7032
E-mail address: jbkim@seoultech.ac.kr
† This paper was presented at the ICMDT2015, Okinawa, Japan, April 2015.
Recommended by Guest Editor Sangho Park

Table 1. Mechanical properties of the bolt and joined part.

Part	Properties	
Bolt (SUS302)	Density (Kg/m^3)	7800
	E (GPa)	200
	ν	0.3
	Plasticity (MPa)	$731+200\varepsilon^{0.5}$
Joined part	Density (Kg/m^3)	1640
	ν	0.41
	E (GPa)	50, 100, 150, 200
	Yield strength (Y_0, MPa)	50, 100, 200, 400
	Hardening (MPa)	$0.1Y_0$

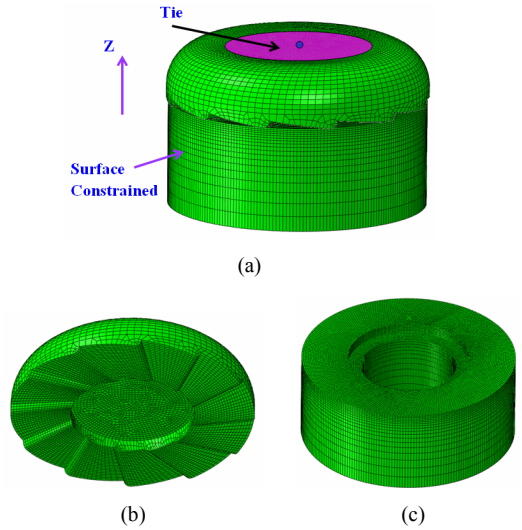

Fig. 1. Finite element analysis model: (a) assembled shape; (b) serrated bolt; (c) joined part.

1 shows the analysis model. Serrations are formed on the bottom side of the bolt head. The threads on the bolt and the bolted part were not modeled for computational effectiveness. By removing the thread shapes from the bolt and bolted part, only the serration effect without the thread effect on the anti-releasing torque can be predicted. All nodes on the flat top surface of the bolt are tied to a center node. The rotational and axial movements of the bolt in the joining and releasing processes are imposed on the tied node as boundary conditions. The bottom side of the bolted part is fixed in axial directions. For all nodes on the side surface of the bolted part, x and y displacements are fixed. An analysis was carried out for various element sizes and the final element size was determined.

An analysis was carried out using the well-known commercial finite element software ABAQUS/Explicit [12]. To overcome the accuracy and instability problem caused by severe deformation, the ALE (Arbitrary Lagrangian-Eulerian) adaptive mesh technique was used. FE analyses were carried out for various mechanical properties, which are listed in Table 1. The bolt is made of SUS202, and its mechanical properties were measured as listed in Table 1. For the joined part, glass-fiber reinforced phenylpropanolamine (PPA-GF50) was used for the inner board of a mobile phone. The density and Poisson ratio of PPA-GF50 were obtained from an online material database [13]. The elastic modulus, tensile yield strength, and Poisson ratio of PPA-GF50 are in the range of 20~50 GPa, 130~170 MPa, and 0.40~0.41, respectively, depending on the production company and detailed grade. Thus, the reference values for the elastic modulus, yield strength, and Poisson ratio were set to 50 GPa, 150 MPa, and 0.41, respectively. Depending on the working temperature and fiber content, thermoplastic materials have a yield strength of 4.0~300 MPa, Poisson ratio of 0.35~0.42, and elastic modulus of 10~120 GPa [13, 14]. To investigate effects of the elastic modulus and yield strength on the anti-releasing performance, FE analyses were carried out for various values of the elastic modulus and yield strength. To investigate the anti-releasing performance when a high stiffness material such as steel was used as a nut, FE analysis was also carried out for the elastic modulus of 200 GPa and tensile yield strength of 400 MPa. Poisson's ratio was fixed to 0.41 to eliminate its effect on the anti-releasing performance.

Both the elastic and plastic deformations were considered in the explicit FE analysis. The time increment was determined based on the density and the elastic modulus of materials. To reduce computational time in FE analysis, acceleration techniques such as mass scaling or time scaling are used in general [15]. In this study, the time scaling technique was used to reduce computational time. Through several preliminary analyses for the joining time, the joining time was determined to be 2.5 ms. A smooth step function was used to reduce the dynamic effect. It was shown that a stable solution was obtained without a dynamic effect, when the joining time was not less than 2.5 ms.

3. Results and discussion

Fig. 2 shows the deformed shape and effective stress distributions after joining and during releasing in case the bolt rotation and axial displacements are 60° and 0.05 mm, respectively. The axial displacement is calculated by using the pitch and the rotation angle. The elastic modulus and yield strength of the bolted part are 50 GPa and 50 MPa, respectively. After joining, it is shown that waves are formed on the top surface of the bolted part due to the serrated bolt. Because most of the element on the top surface of the bolted part deforms plastically, the maximum effective stress is saturated to 60 MPa. The top figure of Fig. 2(b) shows the detailed deformed shape: a kind of obstacle (marked by 'O'). The obstacle plays an important role in increasing the anti-releasing torque.

Fig. 3 shows the joining and releasing torque as rotation angle for various values of yield strength in the case of 50 GPa of the elastic modulus, a 24° rotation, and a 0.02 mm joining depth of the bolt. The bolt is joined up to 24° and released after 24°. The torque is negative during joining and reversed to positive during releasing. As the yield strength increases,

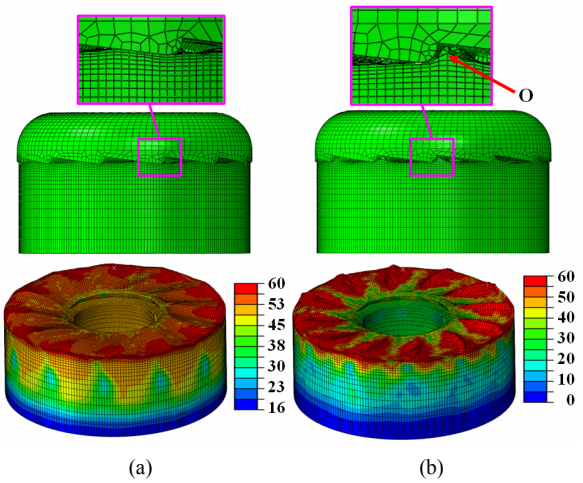

Fig. 2. Deformed shape and effective stress distributions (unit: MPa): (a) after joining; (b) during releasing (60° of rotation and 0.05 mm of joining depth, E_P = 50 GPa, Y_P = 50 MPa).

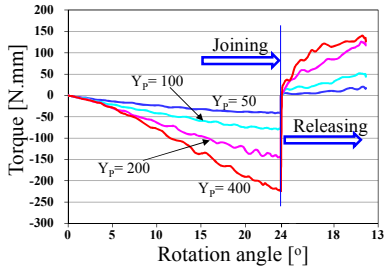

Fig. 3. Joining and releasing torque as rotation angle for various values of yield strength (24° of rotation and 0.02 mm of joining depth, E_P = 50 GPa).

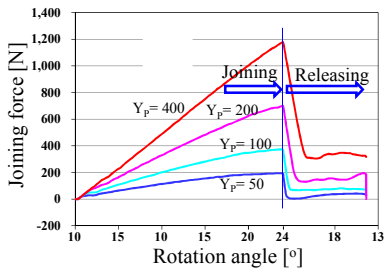

Fig. 4. Joining force as rotation angle for various values of yield strength (24° of rotation and 0.02 mm of joining depth, E_P = 50 GPa).

the maximum joining and anti-releasing torque increase. The joining force as rotation angle for various values of the yield strength is shown in Fig. 4. The other analysis conditions are the same as that of Fig. 3. Because the joining depth is fixed to 0.02 mm, the maximum joining force increases as the yield strength increases. The maximum joining force is used to calculate the anti-release torque of a flat bolt without serration.

Fig. 5 shows the maximum joining torque for various values of the elastic modulus and yield strength. When the joining depth is 0.02 mm, a slight difference in the maximum joining torque between the elastic modulus appears. However, when the joining depth is greater than or equal to 0.03 mm, there is no clear difference in the maximum joining torque for the elastic modulus. Thus, the elastic modulus of the bolted part does not have an effect on the joining torque. However, the maximum joining torque is highly dependent on the yield strength. The maximum joining torque slightly increases as the joining depth increases from 0.02 mm to 0.03 mm and from 0.03 mm to 0.05 mm. Therefore, the effect of the joining depth on the maximum joining torque is insignificant.

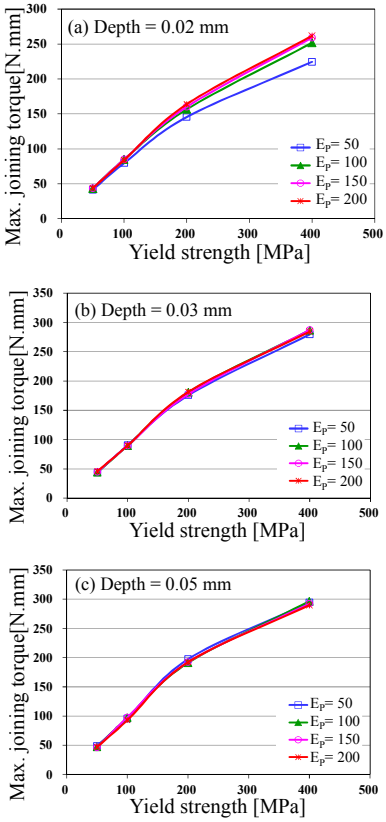

Fig. 5. Maximum joining torque for various values of the elastic modulus and yield strength.

The maximum anti-releasing torque for various values of the elastic modulus and the yield strength is shown in Fig. 6. In contrast to the maximum joining torque shown in Fig. 5, the maximum anti-releasing torque is highly affected by the elastic modulus together with the yield strength. The maximum anti-releasing torque increases as the yield strength decreases. This is because the obstacle to be released, shown in Fig. 2(b), can be formed easily as the elastic modulus deceases. For a comparison of the anti-releasing torque of the serrated bolt, the anti-releasing torque of the flat bolt is also shown. The anti-releasing torque of the flat bolt is calculated using the maximum joining force (see Fig. 4) from Eq. (3).

The joining torque and anti-release torque of the flat bolt are calculated by Eqs. (1) and (2), respectively.

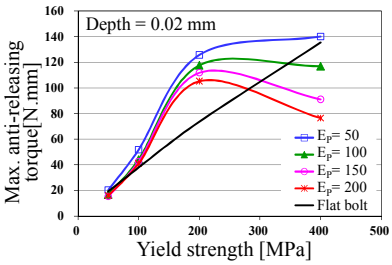

Fig. 6. Maximum anti-releasing torque for various values of the elastic modulus and yield strength.

$$T_J = Q \cdot \left\{ \frac{d_2}{2} \cdot \tan(\rho' + \beta) + \mu_C \frac{d_C}{2} \right\}, \quad (1)$$

$$T_{AR} = Q \cdot \left\{ \frac{d_2}{2} \cdot \tan(\rho' - \beta) + \mu_C \frac{d_C}{2} \right\}, \quad (2)$$

$$T_F = Q\mu_C \frac{d_C}{2}, \quad (3)$$

where, T_J is the joining torque, T_{AJ} is the anti-releasing torque, Q is the joining force, d_2 is the average bolt diameter, d_C is the average collar diameter, ρ' is the equivalent thread friction angle, β is the lead angle, and μ_C is the friction coefficient of the collar. The friction coefficient between metal and plastic is in the range of 0.1~0.3 [16]. The joining and releasing torque is highly affected by the friction. In this analysis, the friction coefficient was set to 0.1, and the resulting torque values were compared relatively. In Eqs. (1) and (2), the first term in the bracket is the torque related to the thread and the second term is related to the friction between the collar and plate. Here, the thread was not modeled, and the joining torque and anti-releasing torque are the same and calculated by Eq. (3). The anti-releasing torque of a flat bolt was calculated for various values of the yield strength using Eq. (3) and plotted in Fig. 6.

When the yield strength of the bolted part is less than or equal to 100 MPa and the joining depth is 0.02 mm, the anti-releasing torque of the serrated bolt is almost the same as that of the flat bolt. Thus, the serration effect is negligible under these conditions. When the yield strength is 200 MPa, the anti-releasing torque is greater than that of the flat bolt. When the yield strength is 400 MPa and the elastic modulus is greater than or equal to 100 GPa, however, the anti-releasing torque is less than that of the flat bolt. These results can be explained from the deformed shape during releasing, as shown in Fig. 7. When the yield strength is 200 MPa, a bump is formed (see Fig. 7(a)) on the bolted part, and this bump plays a role in increasing the anti-releasing torque. However, for the case shown in Fig. 7(b) (E_P = 200 GPa, Y_P = 400 MPa), a bump is not shown and the top surface of the lower part is slightly inclined to the release direction. This inclined surface reduces the anti-releasing torque.

For more quantitative analyses, the serration efficiency is defined by

$$\eta = T_{AR,S} / T_{AR,F}. \quad (4)$$

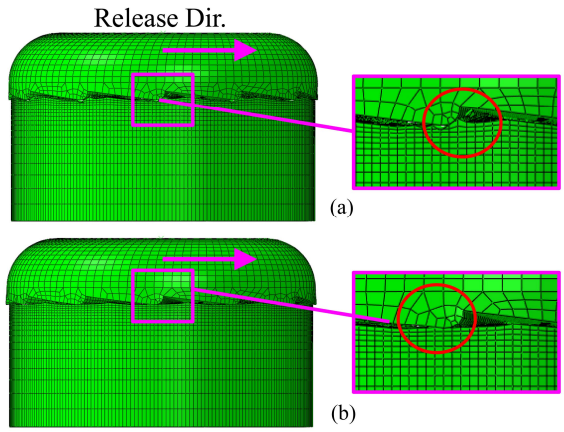

Fig. 7. Deformed shapes during releasing (0.02 mm of joining depth): (a) E_P = 50 GPa, Y_P = 200 MPa; (b) E_P = 200 GPa, Y_P = 400 MPa.

In Eq. (4), η is the serration efficiency and $T_{AR,S}$ and $T_{AR,F}$ are the anti-releasing torque of the serrated bolt and the flat bolt, respectively. Fig. 8 shows the serration efficiency calculated by Eq. (4) for various values of the elastic modulus, yield strength, and joining depth. The results of Fig. 8 can be summarized as follows:

(1) When the joining depth is 0.02 and 0.03 mm, the serration effect is greatest when the yield strength is 200 MPa, and the efficiency increases as the elastic modulus decreases.

(2) When the joining depth is 0.04 and 0.05 mm, the serration efficiency increases as the yield strength decreases.

Using the results shown in Fig. 8, the bolt designer can decide under which conditions the serrated bolt is effective. In addition, the design direction can be obtained by using the results shown in Fig. 8. For example, the elastic modulus and yield strength of a PPA-GF50 plate, which is frequently used in mobile phone boards, are about 18 GPa and 20 MPa, respectively. In this case, when the bolt is joined directly to the plate, as shown in Fig. 9(a), the joining depth should be small due to the fracture of thread of the weak plate. A strong joining torque will cause a fracture of thread of the nut, not the bolt, because the yield strength of the plate is very low. Therefore, this case is similar to the left end point of the blue line in Fig. 8(a) and the serrated bolt is ineffective to increase the anti-releasing torque. To overcome this ineffectiveness, an insert nut with a high strength can be used, as shown in Fig. 9(b). With the high strength of the insert nut, the bolt can be joined in a strong torque. This case is similar to the left end point of the blue line in Fig. 8(d) and the serrated bolt has about 1.7 times anti-releasing torque than the flat bolt.

4. Conclusions

The joining and releasing processes of a serrated bolt were analyzed using the three-dimensional finite element method. An analysis was carried out for various values of the elastic

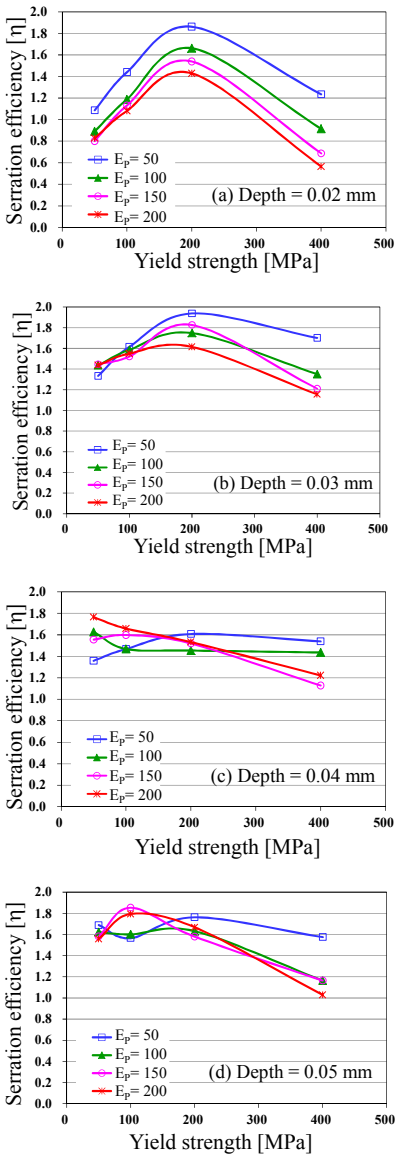

Fig. 8. Efficiency of the serrated bolt for various values of the elastic modulus and yield strength.

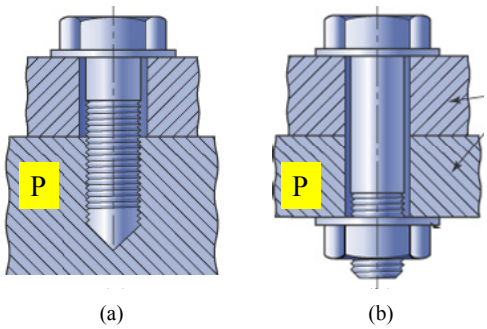

Fig. 9. Two types of bolting methods: (a) direct bolting into a plate; (b) bolting using an insert nut.

modulus and yield strength of the bolted plate, as well as the various joining depths. From the analysis results, the conditions in which the serrated bolt has a great effect on the anti-releasing torque were determined. When a bump, which has a role of becoming an obstacle to the release of a bolt, is formed during releasing, the anti-releasing performance increases. If a weak material is used as a nut, the joining depth should be low to avoid fracture of thread and the serration efficiency is not good. In this case, it is recommended to use an insert nut with a high strength to magnify the serration efficiency.

Acknowledgment

This research was supported by a grant from the Advanced Technology Center (ATC) Program funded by the Ministry of Trade, Industry& Energy of Korea. (No.10045724).

Nomenclature

d_2 : Average thread diameter
d_C : Average collar diameter
Q : Bolt joining force
T_{AR} : Anti-releasing torque
$T_{AR,F}$: Anti-releasing torque of a flat bolt
$T_{AR,S}$: Anti-releasing torque of a serrated bolt
T_F : Joining torque of a flat bolt without thread
β : Lead angle of thread
ρ' : Equivalent friction angle of thread
η : Serration efficiency

References

[1] J. B. Kim, W. S. Seo and K. Park, Damage prediction in the multistep forging process of subminiature screws, *Int. J. Precis. Engng. Manuf.,* 13 (2012) 1619-1624.
[2] Y. Hong, B.-H. Han, B.-J. Kim, D.-P. Hong and Y.-M. Kim, Estimation for bolt fastening conditions of thin aluminum structure using PZT sensors, *J. Mech. Sci. Tech*., 21 (2007) 891-895.
[3] T. Guo, L. Li, L. Cai and Y. Zhao, Alternative method for identification of the dynamic properties of bolted joints, *J. Mech. Sci. Tech*., 26 (2012), 3017-3027.
[4] *http://www.tradeindia.com/fp175751/CHEMICAL-ADHESIVE-FASTENERS.html*.
[5] K. B. Min, J.-B. Kim, K. Park and S. W. Ra, Evaluation of clamping characteristics for subminiature screws according to thread angle variation, *J. Korean Soc. Precis. Eng*., 31 (9) (2014) 839-846.
[6] H.-K. Lee, K. Park, S.-W. Ra and J.-B. Kim, Prediction of joining torque for bit depth of subminiature bolt, *Trans. Korean Soc. Mech. Eng. A*, 38 (8) (2014) 917-923.
[7] N. Sase, S. Koga, K. Nishioka and H. Fuhii, Evaluation of anti-loosening nuts for screw fastener, *J. Mat. Proc. Tech*., 56 (1996) 321-332.
[8] N. Sase, K. Nishioka, S. Koga and H. Fujii, An anti-loosening screw-fastener innovation and its evaluation, *J.*

Mat. Proc. Tech., 77 (1998) 209-215.
[9] A. Bhattacharya, A. Sen and S. Das, An investigation on the anti-loosening characteristics of threaded fastener under vibratory conditions, *Mechanism and Machine Theory*, 45 (2010) 1215-1225.
[10] N. G. Pai and D. P. Hess, Three-dimensional finite element analysis of threaded fastener loosening due to dynamic shear, *Eng. Failure Analysis*, 9 (2002) 383-402.
[11] A. Uzumi, T. Yokoyama, A. Iwasaki and S. Sakai, Three-dimensional finite element analysis of tightening and loosen ing mechanism of threaded fastener, *Eng. Failure Analysis*, 12 (2005) 604-615.
[12] ABAQUS, *ABAQUS manual*, version 6.12, Dassault Systems, USA (2012).
[13] *http://www.matweb.com*.
[14] T. Gao and J. U. Cho, A study on damage and penetration behavior of carbon fiber reinforced plastic sandwich at various impacts, *Int. J. Precis. Engng. Manuf.,* 16 (2015) 1845-1850.
[15] B. Kim, Finite element modeling and parametric study of an automotive V-belt pulley for durability improvement, *Int. J. Precis. Engng. Manuf.,* 16 (2015) 1517-1524.
[16] *http://www.tribology-abc.com/abc/cof.htm*.

Jong-Bong Kim received the B.S. and M.S. in Precision Engineering from KAIST (Korea Advanced Institute of Science & Technology), Daejon, Korea, in 1993 and 1995, respectively. In 2000, he received his Ph.D. in Mechanical Engineering from Taejon, Korea. Since September 2006, he has been with the Department of Automotive Engineering, SeoulTech (Seoul National University of Science & Technology), Seoul, Korea, where became an Associate Professor in 2012. His areas of interest include high-strain rate deformation behaviors of solids and structures, high-strain-rate constitutive equations, penetration analysis of projectiles, active protection systems, and dynamic collision analyses.